Landslides (2017) 14:719–726
DOI 10.1007/s10346-016-0770-y
Received: 23 March 2016
Accepted: 20 October 2016
Published online: 2 November 2016

S. N. Wang · W. Y. Xu · C. Shi · H. J. Chen

Run-out prediction and failure mechanism analysis of the Zhenggang deposit in southwestern China

Abstract Due to the intensive rainfalls in October 2008 and the heavy snowfalls in February 2009, the Zhenggang deposit exhibited a high probability of landslide reactivation. A good understanding in landslide run-out prediction and failure mechanism analysis was thus highly urgent. In this study, the landslide dynamic simulations were performed for studying the run-out prediction and the failure mechanism of the Zhenggang deposit. The impacts of the friction coefficient at sliding surface and the contact damping ratio on landslide run-out were investigated. The potential improvement of the proposed landslide run-out modeling was discussed.

Keywords Landslide run-out prediction · Failure mechanism analysis · Discrete element method (DEM) · The henggang deposit

Introduction

Landslide is one of the most frequently documented geo-disasters, often resulting in enormous loss of properties and human lives (Huang and Chan 2004; Wang et al. 2004; Xie et al. 2014; Xu et al. 2014; Zhu et al. 2013). Mountainous areas in China take 69% of its total territory. About 30 to 35% of the mountainous areas has been or may be threatened by landslide hazards caused by weather conditions, human disturbances, and tectonic activities. An adequate understanding in run-out prediction and landslide failure mechanism is therefore necessary for authorities to specify levels of landslide risk and risk mitigation measures.

In general, landslide stability can be evaluated from two aspects: qualitative research and quantitative analysis (Aleotti and Chowdhury 1999). The qualitative research focuses mainly on geological data, field evidences, and landslide historical information for evaluating the stability of a landslide. However, the subjectivity involved in the selection of both data and rules that govern the stability of a slope tends to be the major limitations of this approach (Guzzetti et al. 1999; Fall et al. 2006; Corominas et al. 2014). The quantitative analysis puts more emphasis on the statistical, mathematical, or numerical analysis of the data that are collected through experiments or geological surveys to study the stability of a landslide (Fall et al. 2006). Data mining and numerical simulation are the most commonly used methods in quantitative analysis. However, although data mining can provide quantitative or semi-quantitative analysis for landslides using machine learning or statistical algorithms, the data collection for a study area, especially over large-scale areas, is always labor-intensive and time-consuming (Jade and Sarkar 1993; Samui and Kothari 2011; Wang et al. 2015). Currently, numerical simulations have been widely used for more accurate landslide analysis (McDougall et al. 2008; Hungr and McDougall 2009; Wang and Sassa 2010; Ishii et al. 2012; Pasenow et al. 2013). The continuum mechanics method is academically more developed and computationally more efficient. So, this method is often used to evaluate the behavior of a slope. However, the approximation of constitutive relations is a weakness. The discrete element method is more widely used in recent years because of its ability to solve discontinuous mechanical problems, especially problems in crack propagation and fracture behavior (Tang et al. 2009; Huang et al. 2012; Jiang and Murakami 2012; Katz et al. 2014). Although it is time-consuming to run a model containing hundreds of thousands of elements, the ability to consider large deformation is a great advantage over the continuum analysis approach. The discrete element method is therefore more applicable to analyze landslide run-out predictions. In this study, both 2D and 3D numerical run-out models of the Zhenggang deposit were established by the particle flow codes (PFC). The run-out prediction and the failure mechanism of the landslide deposit were analyzed. The characteristics of the landslide run-out under different influence factors were also discussed.

Overview of the Zhenggang deposit

Topographic and geomorphologic features

The Zhenggang deposit (E98° 47′–98° 98′, N28° 33′–29° 10′) is an ancient complex landslide, located at southeastern Tibetan Plateau, China, as shown in Fig. 1a. Due to the intensive rainfalls in October 2008 and the heavy snowfalls in February 2009, previous signs of a new landslide such as surface cracks, bulging deformations, and minor scarps were observed, as shown in Fig. 1b. All these signs indicate that the Zhenggang deposit at that time showed a high probability of landslide reactivation. Although the Zhenggang deposit went into a metastable state after implementing the dewatering measures, the huge volume of the Zhenggang deposit with a potentially high movement velocity has always been a great threat to the residents and the construction and operation of the Gushui Hydropower Station.

Figure 2a shows that the crown of the main landslide scarp of the Zhenggang deposit turns on a shape of a round-backed armchair on a plane. Three main gullies—upstream gully, Zhenggang gully, and Yagong gully—scatter on the slope surface, as shown in Fig. 2b. The Zhenggang gully was exposed to intense gully erosion, leading to the deepest cutting depths. Therefore, the whole Zhenggang deposit can be divided into two subdomains in geomorphologic structure. The upstream subdomain, Zone-I, lies mainly between the upstream gully and the Zhenggang gully, with a volume of about 9.4 million cubic meter. The downstream subdomain, Zone-II, lies mainly between the Zhenggang gully and the Yagong gully, with a volume of about 38.1 million cubic meter. The whole Zhenggang deposit has an elevation of 2180 to 3220 m a.s.l. and a width of about 1300 m. Natural vegetation develops well above the elevation of 2500 m a.s.l.

Geological and hydrological conditions

It can be seen from Fig. 2c, d that the Zhenggang deposit is composed of three layers in geological profile: landslide deposit, interlayered clay (slip zone), and bedrock. The landslide deposit ranging in depth from 26.9 to 34.5 m consists of diluvium deposit

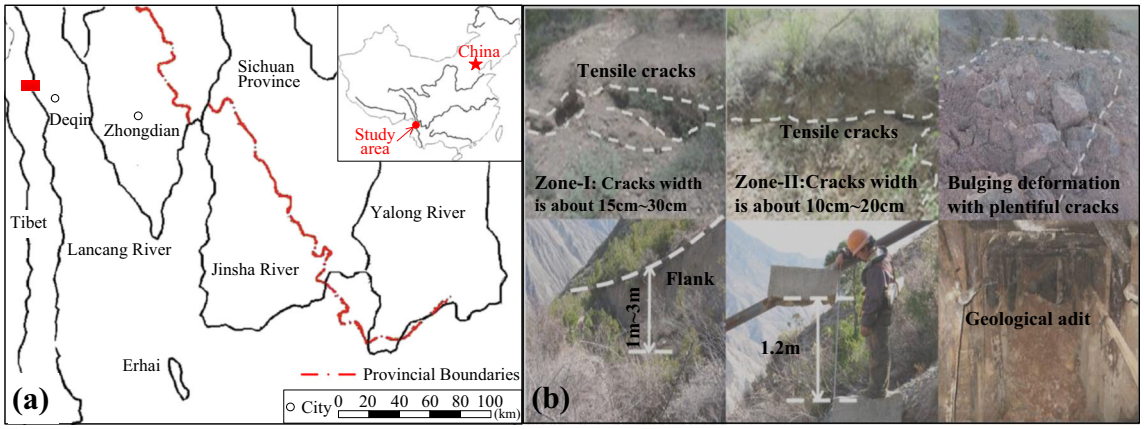

Fig. 1 Site location and landslide premonitions of the Zhenggang deposit

of Quaternary System (Q^{dl}), glaciofluvial deposit of Holocene series (Q^{fgl}), and landslide deposit (Q^{del}). The material of the landslide deposit is a chaotic mixture of fine sandy soil and lumps of weathered basalt boulders ranging in size from a few centimeters to more than 20 m. Because of the unconsolidated features of the landslide deposit, atmospheric precipitation and snow melting water can infiltrate into the landslide deposit rapidly, imposing hydrodynamic pressure on the landslide body and decreasing the shear strength of the interlayered clay. The slip zone, located between the landslide deposit and the bedrocks as shown in Fig. 3, has a thickness varying from 1 to 3 m. The material of the slip zone is amaranthine or off-white fine clay, mingled with fine gravels. Due to a low shear strength and permeability of clay, the slip zone plays a significant role in pore water pressure development and landslide stability when abundant water enters into the landslide deposit. The bedrock underlying the slip zone consists of argillaceous-calcareous slates and siltstones, presenting strong unloading and toppling deformation features as shown in Fig. 2c, d. The lithology of the bedrock near the toe of the rupture surface is weathered basalts. Geological surveys indicate that the rupture

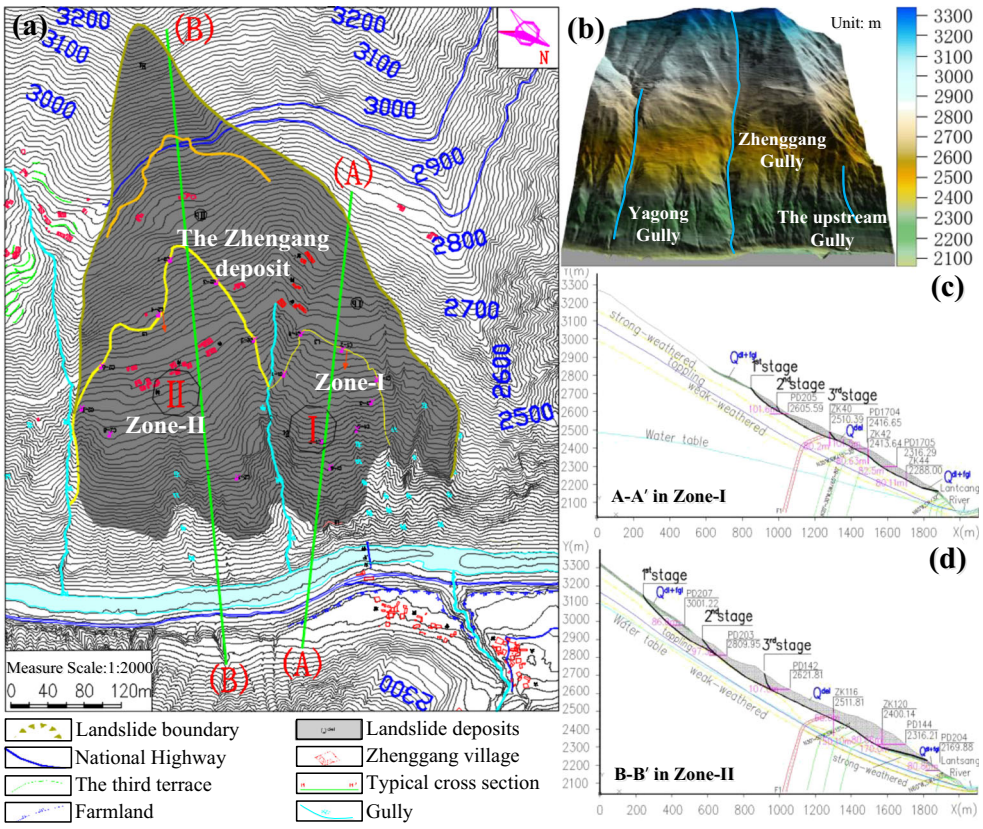

Fig. 2 Topographic and geomorphologic map (**a**) and typical cross sections (**b**) of the Zhenggang deposit

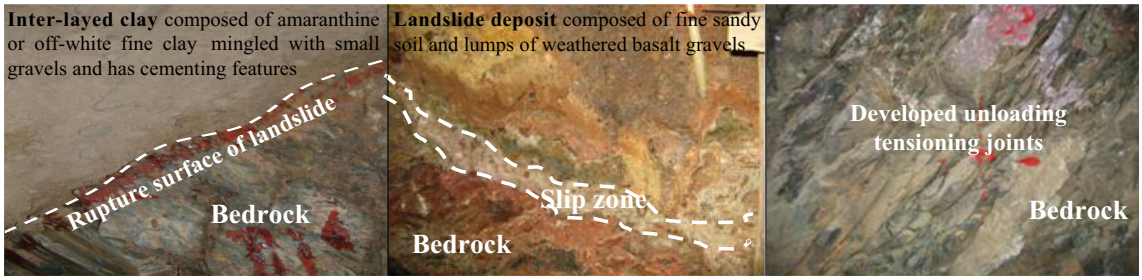

Fig. 3 A view on a stratigraphic contact of the Zhenggang deposit

surface of the Zhenggang deposit spreads mainly along the interlayered clay and sinks inward overall. The inclination of the rupture surface is about 40°–55° near the top, 20°–40° in the middle of the slope, and relatively gentle near the toe. The shape of the rupture surface looks approximately like a spoon. Slickensides orienting downward the slope are visible on the upper surface of the slip zone. The groundwater table is commonly below the interlayered clay, so the influence of underground water on the landslide behavior is not considered in this study.

Landslide run-out predictions

Landslide run-out prediction method

Particle flow code (PFC), proposed by Cundall and Strack (1979), is an advanced multi-threaded discontinuum code which can be used to simulate the instability process and the run-out of a landslide on condition that the body of the landslide can be seen as an assembly of a finite number of spherical particles with size much smaller than the slope itself; the collisions between particles or between particles and sliding surfaces are idealized as inelastic collision, and the lift and drag of air is not taken into consideration (Itasca 2006; Poisel and Preh 2008). So in this study, PFC2D/3D was used to study the landslide run-out and the failure mechanism of the Zhenggang deposit.

Landslide run-out modeling and material parameters setting

The 3D sliding surface of the Zhenggang deposit in this study was modeled by 15,642 face elements, and the landslide deposit was modeled by 55,284 ball elements with radii ranging from 4.0 to 6.0 m, as shown in Fig. 4a. Figure 4b shows 2D run-out models for two typical cross sections of the Zhenggang deposit. The size of the particles in the 2D and 3D models is the same.

At present, there is still no straightforward theoretical solution on how to transform the macroparameters into corresponding mesoparameters because of the fact that the macroscopic behavior of a granular medium is mainly determined by the contact mechanical properties of a material. The relationship between mesoparameters and mechanical characteristics of a real problem is thus always a focal point of a study (Potyondy and Cundall 2004). Yoon (2007), Fakhimi and Villegas (2007), and Cho et al. (2007) had proposed an experimental design and optimization for PFC model calibration. So, in this study, numerical compression tests for calibrating the mesomechanical parameters from the macroscopic parameters of the landslide deposit were conducted

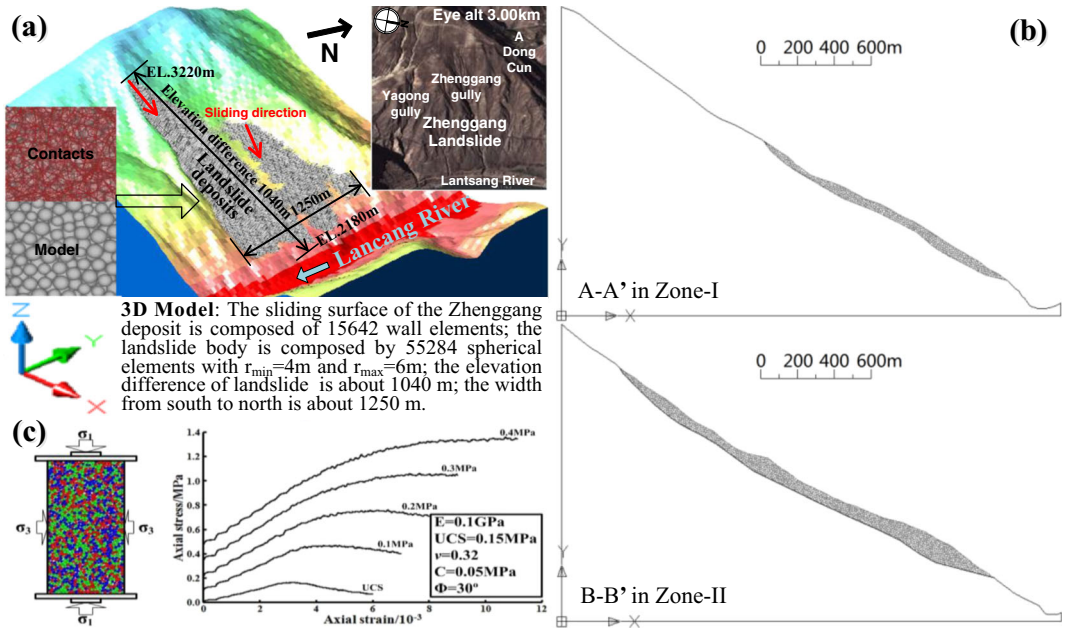

Fig. 4 PFC models and parameter calibration for landslide run-out predictions

Table 1 Numerical parameters of the PFC models

Parameters of spherical elements				Parameters of facets	
Normal stiffness (GN/m)	0.2	Shear stiffness (GN/m)	0.2	Normal stiffness (GN/m)	2.0
Parallel bond normal stiffness (MN/m)	10.0	Parallel bond shear stiffness (MN/m)	10.0	Shear stiffness (GN/m)	2.0
Parallel bond normal strength (MN)	0.5	Parallel bond shear strength (MN)	0.35	Friction coefficient	0.5
Parallel bond radius	0.8	Friction coefficient	0.5		
Minimum radius (m)	4.0	Rmax/Rmin	1.5		

by trial and error, as shown in Fig. 4c. The numerical compression model used the same particle size as those in the landslide run-out modeling. The numerical mesoparameters of the landslide deposit are shown in Table 1.

In addition, although local damping ratio is applicable to establish equilibrium and to conduct quasi-static deformation simulations, energy dissipation caused by free flight of particles and/or impacts between particles is more significantly affected by viscous contact damping. Hence, in this study, the local damping ratio α is 0.5, the viscous damping ratios are $c_n = 0.10$ and $c_s = 0.08$ as referenced from the research by Zhang et al. (2012).

3D run-out predictions of the Zhenggang deposit

In order to illustrate the kinematic failure process of the Zhenggang deposit, the calibrated material mesoparameters weakened by 20% were considered as relevant parameters for triggering a landslide. Such a consideration was made based on the following two aspects: (1) some literature reported that the residual strength of rupture surfaces is commonly very low, with cohesion equal to zero, and internal friction angle between 10° and 25° (Cai et al. 2007; Hoek and Bray 1981; Fell et al. 1987). For the Zhenggang deposit, the internal friction angle of the interlayered clay is about 26.5°. If the internal friction angle is weakened for 20%, it would be lower than the upper value of 25°. (2) The geological survey indicates that the Zhenggang deposit is in a metastable status. A slight reduction of the shear strength or an unexpected external disturbance would cause the slope failure. So, weakening for 20% of the shear strengths of the interlayered clay and the landslide deposit is sufficient to trigger a landslide. Figure 5 presents the 3D landslide run-out predictions of the Zhenggang deposit at different time in spite of no consideration of the viscous contact damping. It is visible that when the landslide deposit starts to slide, the landslide deposit in Zone-I slides towards to the Zhenggang gully and the river valley, while the landslide deposit in Zone-II slides to the river valley. The lateral spreads of the Zhenggang deposit are restrained by the mountain ridges above the elevation of 2200 m a.s.l. But below the elevation of 2200 m a.s.l., the lateral restriction effect weakened gradually and the landslide deposit slides rapidly downward to the Lancang River with growing lateral spread. The landslide deposit blocks the river quickly and re-stabilizes eventually with a funnel-shaped distribution. Figure 6a, b show that the landslide forms the main framework of accumulation topography in a short time. The maximum velocity of the whole landslide deposit reaches to

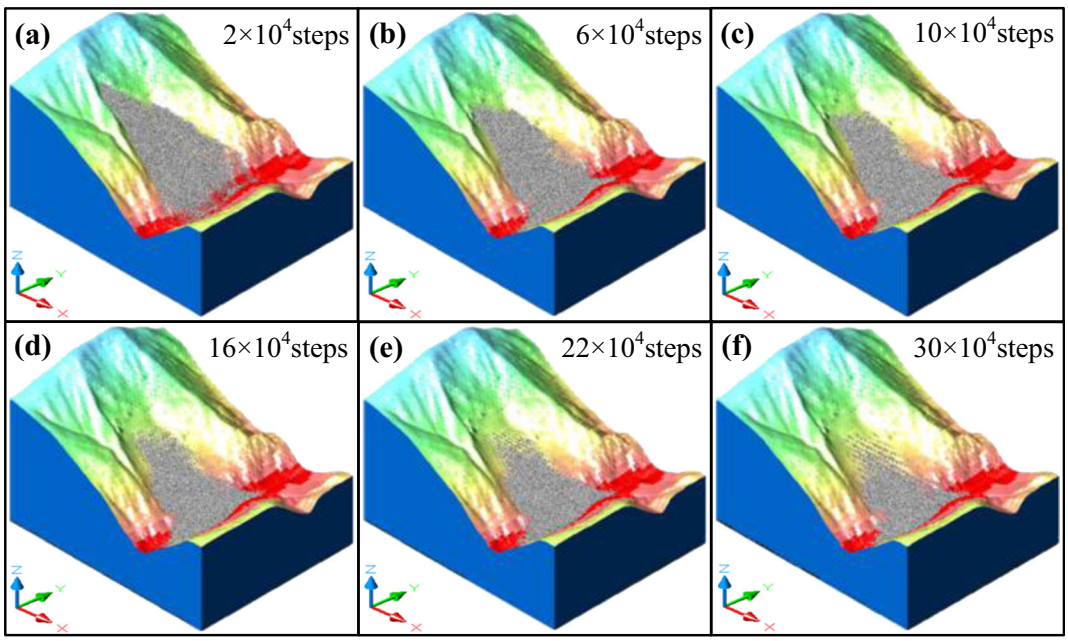

Fig. 5 3D run-out predictions for the Zhenggang deposit in time

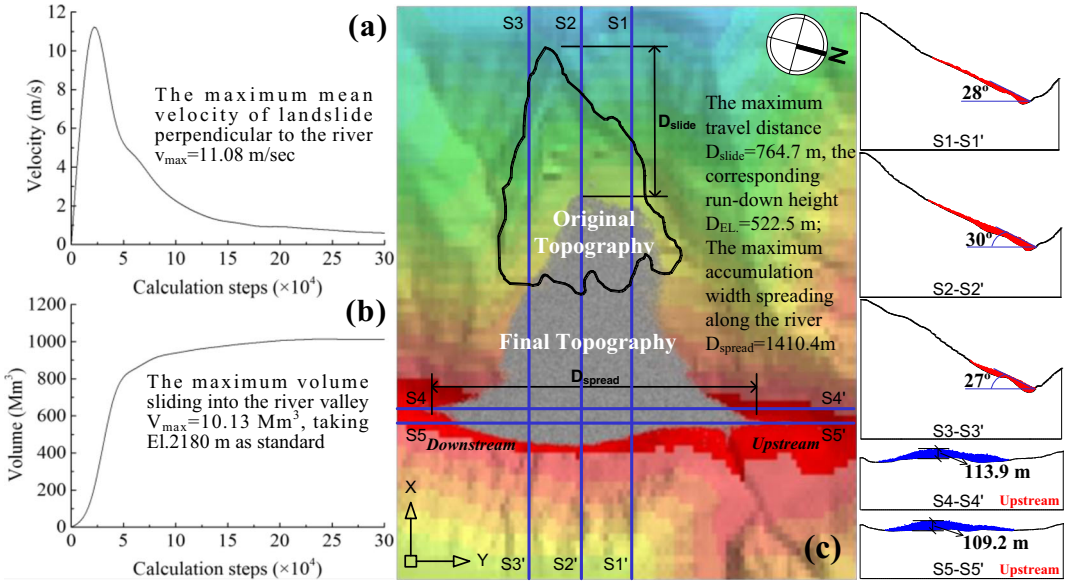

Fig. 6 Time history curves of collapsed volume (**a**) and movement velocity (**b**), and accumulation features (**c**) after the landslide occurs.

11.08 m/s. Figure 6c shows that the topography of the landslide deposit changes dramatically after sliding. The elevation of the landslide deposit decreases approximately 522.5 m a.s.l. The travel distance of the landslide deposit perpendicular to the Lancang River is about 764.7 m. The coverage area of the landslide deposit expands. The width of the accumulation area along the Lancang River is about 1410.4 m. The average inclination and the maximum thickness of the final landslide accumulation topography are about 28° and 113.9 m, respectively. So the failure of the Zhenggang deposit is quite likely to be a catastrophic landslide due to its high speed and huge volume.

Failure mechanism analysis of the Zhenggang deposit

Figure 7 shows that as the deformation develops the bond failures (due to tension and shear) within the landslide deposit increase dramatically, especially in Zone-II. The distributions of local bond failures and the deformation between the upper and lower parts of the landslide deposit indicate that there shall be a significant compressional deformation occurring at the upper part in Zone-II. According to the distribution of activity, the landslide in Zone-II should be an advancing landslide (WP/WLI 1993). A few amount of local bond failures at the upper part, the early crack extensions at the middle part, and the evident

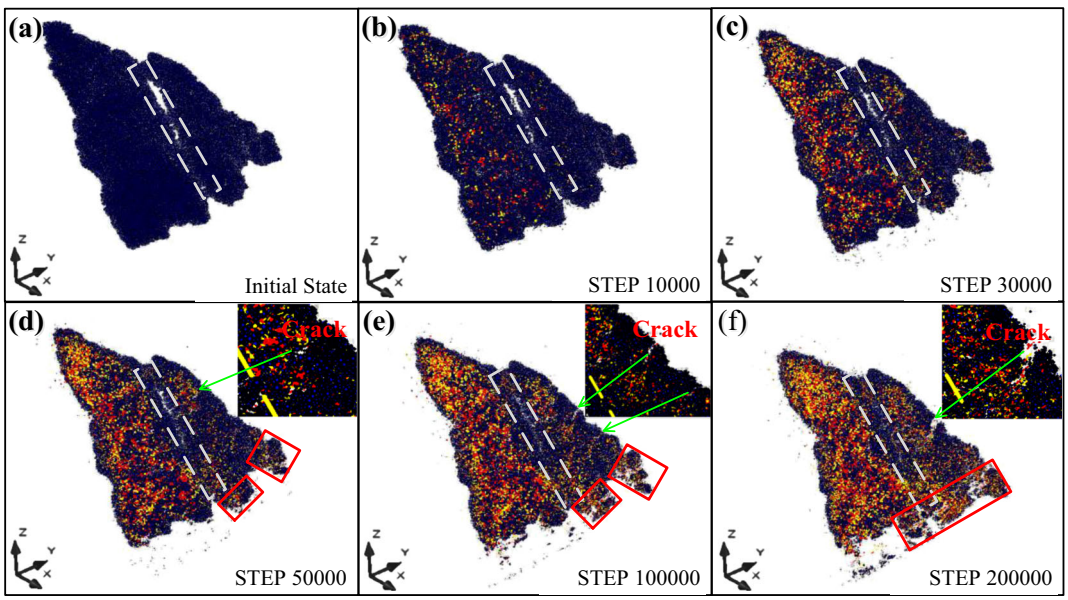

*Yellow and red bars indicate bond failures due to tension and shear, the regions marked by dashed boxes are the Zhenggang gully, and the regions marked by solid boxes are the foot of the landslide.

Fig. 7 Distributions of bond failures and propagation of cracks with increasing deformation

collapses near the toe of the landslide deposit in Zone-I indicate that the failure of the landslide deposit in Zone-I would probably induce by the loss of support from the lower part. According to the distribution of activity, the landslide in Zone-I should be a retrogressive landslide (WP/WLI 1993). The same conclusions can also be reached from the 2D run-out simulations, as shown in Fig. 8. Figure 8a–f illustrates that when the bond failures in Zone-I spread to the lower part (See A_1), the landslide deposit near the toe in Zone-I collapses first. But the deformation in Zone-I at the upper part is not obvious at the early stage of the landslide failure (See A_2). When the middle and upper parts of the landslide deposit in Zone-I lose the support from the lower part of the landslide deposit, the landslide deposit in Zone-I loses its original stability. So, the conclusion on the distribution of activity of the landslide deposit in Zone-I, gained from the 3D run-out analysis, is reasonable. The landslide deposit in Zone-I shall be displaced along the rupture surface with an inclination of 27° eventually. Figure 8g–l shows that when the landslide deposit appears instability, the bond failures in Zone-II spread quickly along the rupture surface (See B_1). However, due to the steep slope gradient of the rupture surface at the upper part in Zone-II, the deformation in Zone-II at the upper part is more obvious than that at the

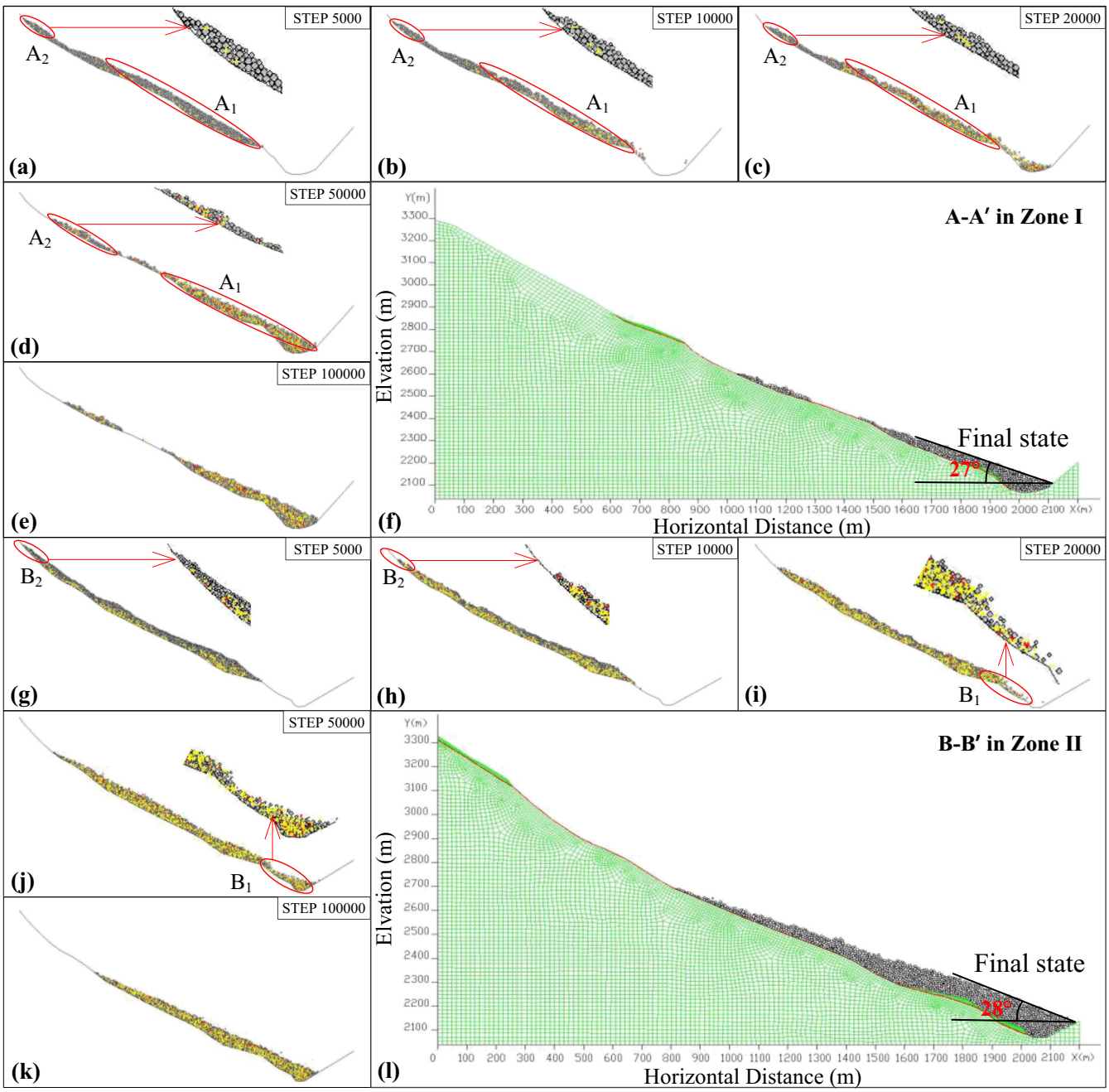

*Yellow and red bars indicate bond failure due to tension and shear.

Fig. 8 2D run-out predictions for the Zhenggang deposit in time

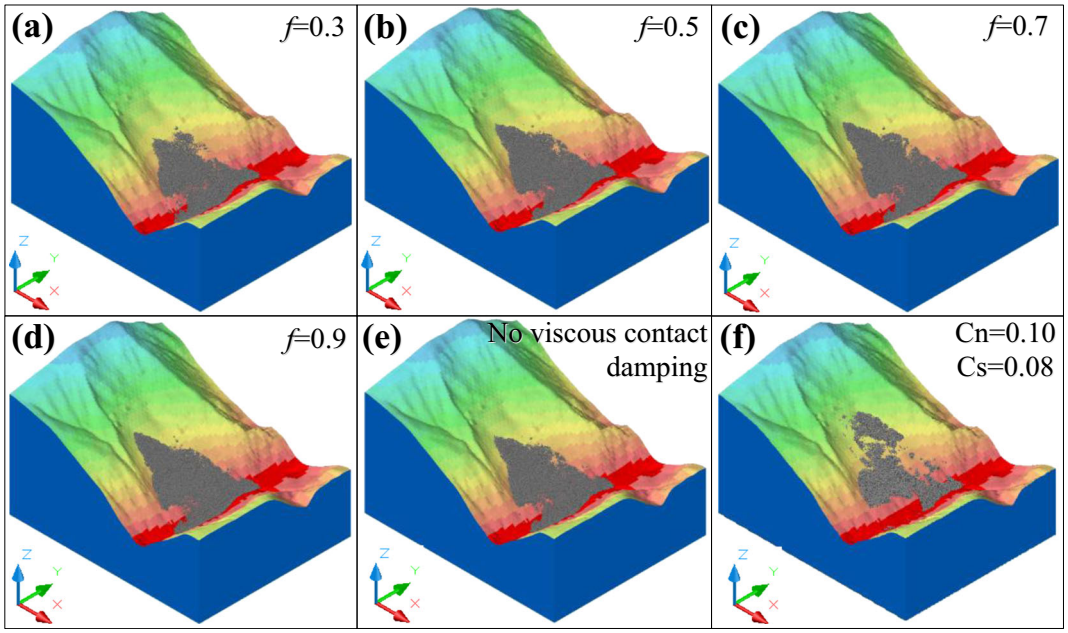

Fig. 9 Landslide run-out predictions under different friction coefficients and viscous contact damping

middle and lower parts. When the accumulated plastic deformation in Zone-II at the upper part reaches a certain level, the landslide deposit in Zone-II at the upper part begins to slide down to the middle part, which results in significant compressional deformation occurring at the lower parts and remarkably disintegration at the foot of the landslide. So according to the distribution of activity, the landslide in Zone-II should be an advancing landslide. The landslide deposit in Zone-II shall be displaced along the rupture surface with an inclination of 28° in final.

Discussion

Impacts of friction coefficient at sliding surface on run-out features

In general, the mechanical properties of soil at the sliding surface are crucial for landslide stability. The poorer properties of material at the sliding surface will cause the greater magnitude of landslide. In this study, landslide run-out predictions related to different friction coefficients at the sliding surface were carried out, where viscous damping ratios of all contacts were set to zero for reducing computing time. Results shown in Fig. 9a–d present that both travel distance and run-down height (the elevation difference of the top of the landslide before and after sliding) decrease with the increasing of the friction coefficient.

Impacts of viscous contact damping on run-out features

Figure 9e, f shows the results of landslide run-out predictions related to different values of viscous contact damping. Results of analyses indicate that the magnitude of landslide disintegration is sensitive to the value of viscous contact damping. The greater value of the viscous contact damping will cause more landslide deposit laid on where the slope gradient of the rupture surface is gentle. So, a reasonable value of viscous contact damping can reflect the response of a landslide more realistically.

Potential improvement on landslide run-out modeling

Although the method proposed in this study can simulate the occurrence and the dynamic development of a landslide for better understanding in landslide's failure mechanism, three issues remain to be improved.

(a) The clay interlayer is actually the dominant precausing factor that influences on the stability of landslide. For the accurate landslide forecast, it would be necessary to consider the impacts of the cohesion and the hydraulic characteristics of the interlayered clay on the landslide stability.
(b) A rise of groundwater table may decrease the normal stresses on the rupture surface and reduce the effective shear strength of the interlayered clay, leading to increasing landslide risk. The influence of groundwater on landslide should be taken into account, especially for landslides in reservoir areas.
(c) The landslide deposit is a mixture of fine grained soil and gravel. The coarse-sized gravels tend to have an anchoring effect in the increasing of the stability of landslide. The uncertainty of landslide stability induced by the existence of internal gravels remains a future study topic.

Conclusion

The Zhenggang deposit is a complex large-scale landslide. The landslide run-out predictions indicate that once the Zhenggang deposit loses stability, the landslide deposit will block the Lancang River quickly with a funnel-shaped distribution. The distribution of activity of the landslide deposit is a retrogressive landslide in Zone-I and an advancing landslide in Zone-II which agrees with the preliminary conclusions gained from landslide premonitions and field geological surveys. Outcomes also indicate that the poorer properties of material at the sliding surface will cause the greater magnitude of landslide, and the greater value of the viscous contact damping will cause more landslide

deposit laid on where the slope gradient of the rupture surface is gentle.

Acknowledgments

The research work was supported by the National Key Technology R&D Program of China (2013BAB06B00), the National Natural Science Foundation of China (50911130366; 51309089), and the Fundamental Research Funds for the Central Universities of China. (KYLX_0441).

References

Aleotti P, Chowdhury R (1999) Landslide hazard assessment: summary review and new perspectives. B Eng Geol Environ 58:21–44

Cai M, Kaiser PK, Tasaka Y, Minami M (2007) Determination of residual strength parameters of jointed rock masses using the GSI system. Int J Rock Mech Min 44:247–265

Cho NA, Martin CD, Sego DC (2007) A clumped particle model for rock. Int J Rock Mech Min 44:997–1010

Corominas J, Van Westen C, Frattini P, Cascini L, Malet JP, Fotopoulou S, Catani F, Van Den Eeckhaut M, Mavrouli O, Agliardi F, Pitilakis K (2014) Recommendations for the quantitative analysis of landslide risk. B Eng Geol Environ 73:209–263

Cundall PA, Strack OD (1979) A discrete numerical model for granular assemblies. Geotechnique 29:47–65

Fakhimi A, Villegas T (2007) Application of dimensional analysis in calibration of a discrete element model for rock deformation and fracture. Rock Mech Rock Eng 40:193–211

Fall M, Azzam R, Noubactep C (2006) A multi-method approach to study the stability of natural slopes and landslide susceptibility mapping. Eng Geol 82:241–263

Fell R, MacGregor JP, Williams J, Searle P (1987) A landslide in Patonga claystone on the Sydney-Newcastle freeway. Geotechnique 37:255–269

Guzzetti F, Carrara A, Cardinali M, Reichenbach P (1999) Landslide hazard evaluation: a review of current techniques and their application in a multi-scale study, Central Italy. Geomorphology 31:181–216

Hoek E, Bray JD (1981) Rock slope engineering. CRC Press, New York

Huang R, Chan L (2004) Human-induced landslides in China: mechanism study and its implications on slope management. CJRME 23:2766–2777 (In Chinese)

Huang Y, Zhang W, Xu Q, Xie P, Hao L (2012) Run-out analysis of flow-like landslides triggered by the Ms 8.0 2008 Wenchuan earthquake using smoothed particle hydrodynamics. Landslides 9:275–283

Hungr O, McDougall S (2009) Two numerical models for landslide dynamic analysis. Comput Geosci 35:978–992

Ishii Y, Ota K, Kuraoka S, Tsunaki R (2012) Evaluation of slope stability by finite element method using observed displacement of landslide. Landslides 9:335–348

Itasca (2006) PFC3D User's Manual. Itasca Consulting Group, Inc, Minneapolis, MN, USA

Jade S, Sarkar S (1993) Statistical models for slope instability classification. Eng Geol 36:91–98

Jiang M, Murakami A (2012) Distinct element method analyses of idealized bonded-granulate cut slope. Granul Matter 14:393–410

Katz O, Morgan JK, Aharonov E, Dugan B (2014) Controls on the size and geometry of landslides: insights from discrete element numerical simulations. Geomorphology 220:104

McDougall S, Pirulli M, Hungr O, Scavia C (2008) Advances in landslide continuum dynamic modeling. In: Chen Z, Zhang J, Ho K, Wu F, Li Z (eds) Proceedings of the 10th international symposium on landslides and engineered slopes, Xi'an, China. CRC Press, Boca Raton, pp. 145–157

Pasenow F, Zilian A, Dinkler D (2013) Extended space-time finite elements for landslide dynamics. Int J Numer Meth Eng 93:329–354

Poisel R, Preh A (2008) 3D landslide run out modelling using the particle flow code PFC3D. In: Chen Z, Zhang J, Li Z, Wu F, Ho K (eds) Proceedings of the 10th international symposium on landslides and engineered slopes, Xi'an, China. CRC Press, Boca Raton, pp. 873–879

Potyondy DO, Cundall PA (2004) A bonded-particle model for rock. Int J Rock Mech Min 41:1329–1364

Samui P, Kothari DP (2011) Utilization of a least square support vector machine (LSSVM) for slope stability analysis. Sci Iran 18:53–58

Tang CL, Hu JC, Lin ML, Angelier J, Lu CY, Chan YC, Chu HT (2009) The Tsaoling landslide triggered by the Chi-Chi earthquake, Taiwan: insights from a discrete element simulation. Eng Geol 106:1–19

Wang F, Sassa K (2010) Landslide simulation by a geotechnical model combined with a model for apparent friction change. Phys Chem Earth A B C 35:149–161

Wang FW, Zhang YM, Huo ZT, Matsumoto T, Huang BL (2004) The July 14, 2003 Qianjiangping landslide, Three Gorges Reservoir, China. Landslides 1:157–162

Wang YT, Seijmonsbergen AC, Bouten W, Chen QT (2015) Using statistical learning algorithms in regional landslide susceptibility zonation with limited landslide field data. J Mt Sci 12:268–288

WP/WLI (1993) A suggested method for describing the activity of a landslide. Bull Int Assoc Eng Geol 47:53–57

Xie NM, Xin JH, Liu SF (2014) China's regional meteorological disaster loss analysis and evaluation based on grey cluster model. Nat Hazards 71:1067–1089

Xu L, Meng X, Xu X (2014) Natural hazard chain research in China: a review. Nat Hazards 70:1631–1659

Yoon J (2007) Application of experimental design and optimization to PFC model calibration in uniaxial compression simulation. Int J Rock Mech Min 44:871–889

Zhang L, Huiming T, Chengren X (2012) Movement process simulation of high-speed longdistance Jiweishan landslide with PFC 3D. CJRME 31:2601–2611 (In Chinese)

Zhu SB, Shi YL, Lu M, Xie FR (2013) Dynamic mechanisms of earthquake-triggered landslides. Sci China Earth Sci 56:1769–1779

S. N. Wang · W. Y. Xu · C. Shi · H. J. Chen
Key Laboratory of Ministry of Education for Geomechanics and Embankment Engineering,
Hohai University,
Nanjing, 210098, China

S. N. Wang (✉) · W. Y. Xu · C. Shi · H. J. Chen
Institute of Geotechnical Engineering,
Hohai University,
Nanjing, 210098, China
e-mail: shengnian.wang@foxmail.com